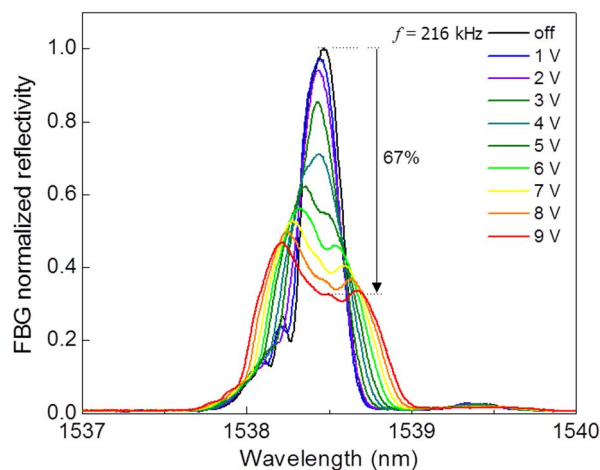


# Reflectivity and Bandwidth Modulation of Fiber Bragg Gratings in a Suspended Core Fiber by Tunable Acoustic Waves

Volume 6, Number 6, December 2014

Ricardo E. Silva  
Martin Becker  
Alexander Hartung  
Manfred Rothhardt  
Alexandre A. P. Pohl  
Hartmut Bartelt



DOI: 10.1109/JPHOT.2014.2366161  
1943-0655 © 2014 IEEE

# Reflectivity and Bandwidth Modulation of Fiber Bragg Gratings in a Suspended Core Fiber by Tunable Acoustic Waves

Ricardo E. Silva,<sup>1,2,3</sup> Martin Becker,<sup>1</sup> Alexander Hartung,<sup>1</sup>  
Manfred Rothhardt,<sup>1</sup> Alexandre A. P. Pohl,<sup>3</sup> and Hartmut Bartelt<sup>1,2</sup>

<sup>1</sup>Leibniz Institute of Photonic Technology (IPHT), 07702, Jena, Germany

<sup>2</sup>Friedrich Schiller University Jena (FSU), 07743, Jena, Germany

<sup>3</sup>Federal University of Technology-Paraná (UTFPR), 80230-901 Curitiba, Brazil

DOI: 10.1109/JPHOT.2014.2366161

1943-0655 © 2014 IEEE. Translations and content mining are permitted for academic research only.  
Personal use is also permitted, but republication/redistribution requires IEEE permission.  
See [http://www.ieee.org/publications\\_standards/publications/rights/index.html](http://www.ieee.org/publications_standards/publications/rights/index.html) for more information.

Manuscript received August 8, 2014; revised October 14, 2014; accepted October 16, 2014. Date of publication November 3, 2014; date of current version November 14, 2014. This work was supported in part by the Thuringian Ministry of Education, Science, and Culture (EFRE program); by the Coordenação de Aperfeiçoamento de Pessoal de Nível Superior (CAPES); by the Ministério da Defesa—Projeto Pró-Defesa; and by the CNPq/FAPESP—INCT (FOTONICOM). Corresponding author: R. E. Silva (e-mail: ricardoezq@yahoo.com.br).

**Abstract:** The acousto-optic modulation of fiber Bragg gratings in a four-hole suspended core fiber is experimentally demonstrated. Strong modulations with a reflectivity amplitude decrease by up to 67% and a 57% bandwidth increase in the Bragg resonance are obtained for gratings of 0.26- and 1-nm 3-dB bandwidths, respectively. The reduction of the required acoustic power for achieving the acousto-optic modulation compared to conventional solid-core single-mode fibers points to more efficient modulator devices in suspended core fibers.

**Index Terms:** Acousto-optic devices, fiber Bragg gratings, microstructured fibers.

## 1. Introduction

Bandwidth and reflectivity modulation of fiber Bragg gratings (FBGs) is of interest for applications in dispersion compensators, fiber lasers, optical pulse sources, and bandpass filters [1]–[7]. Temperature based techniques have been proposed to induce dynamic chirp in FBGs since they allow the electrical control of the grating properties [3], [4]. However, the device response time is also limited because the material heating-cooling process is relatively slow. In addition, the low sensitivity of the silica thermo-optic coefficient requires high temperatures to produce small spectral variations in the nanometer range.

Strain based techniques provide broader wavelength tuning range and faster response time compared to gradient temperature techniques [8]. Among the available techniques, fiber with S-shape bending allows chirping the FBG without causing the central wavelength shift [5]–[7]. The fiber is embedded on a thin and flexible metal beam, which is subjected to two antisymmetric curvatures. The grating center is fixed at the midpoint of the S-bending, where no strain is applied and, therefore, at this point the Bragg wavelength is not disturbed. On one side of the curvature, the tension strain shifts the reflection spectrum to longer wavelengths, whereas on the other side, the compression strain shifts it to shorter wavelengths. Thus, the grating spectral bandwidth is increased, but the center wavelength remains unchanged. However, S-bent devices

have limitations for the dynamic and fast control of the FBG spectrum, since they are often mechanically driven. In contrast, acousto-optic devices allow the fast control of the elasto-optic FBG properties by electrically tunable acoustic waves [1], [9]–[14]. In particular, the interaction of longitudinal acoustic waves and Bragg gratings allows the dynamic change of the reflectivity and the wavelength of reflection bands on both sides of the Bragg resonance, which is useful for the control of tunable reflectors, modulators and fiber lasers [9]–[11]. Moreover, the superposition between flexural and longitudinal acoustic waves can be applied to induce chirp in the grating, which is useful to modulate the Bragg resonance reflectivity and the spectrum bandwidth [15].

However, the acoustic power is generally distributed over the whole fiber cross section in standard single mode fibers (SMFs), which reduces the overlap between the acoustic wave and the grating inscribed in the fiber core, and consequently, the acousto-optic interaction. Cladding-etched fibers with strong gratings or tapered fibers with long gratings enhance the acousto-optic interaction [9]–[11], but the inscription of strong gratings requires high laser power densities, high germanium dopings or hydrogen loading [16]. Moreover, the inscription of long gratings is limited by the spatial and temporal coherence of employed interferometry techniques or requires the use of long phase masks or additional equipment to shift the fiber or the laser beam [17]. The realization of tapers requires also specific equipment, mainly due to the relatively long fiber transitions required to increase the acousto-optic interaction. In addition, the reduction of the fiber diameter affects its mechanical stability and makes the optical properties more susceptible to surface contamination.

One promising option, besides the above mentioned techniques, is the use of suspended-core fibers (SCFs) [18]–[21]. These fibers present a very small core in size of a few micrometers suspended by thin radial walls, and surrounded by a single ring of large air holes. This allows a significant reduction of the amount of silica in the cladding, which leads to a larger acousto-optic interaction between the acoustic wave and the grating in the core. In this work, we experimentally investigated the reflectivity modulation of two gratings inscribed in a four holes suspended-core fiber. By changing the acoustic power, we verified that the grating reflectivity can be significantly modulated compared to results obtained with standard fibers used in previous works. In addition, the grating bandwidth can be increased, while correcting the spectrum envelope to an almost Gaussian shape. The results indicate larger acousto-optic effects in suspended-core fibers, which is desirable to reduce the size and the power consumed by acousto-optic devices. It also relaxes the requirements for inscribing strong or long gratings as shorter gratings can be employed, and avoids the cladding reduction by etching or taper techniques.

## 2. Theory

The interaction of longitudinal acoustic waves and fiber Bragg gratings induces reflection bands in both sides of the Bragg resonance. Fig. 1 illustrates the principle of this acousto-optic interaction. When an optical mode with effective index  $n_{\text{eff}}$  propagates in a non-perturbed fiber containing a grating of period  $\Lambda$ , this mode will be reflected in the grating, resulting in a reflected band at the Bragg wavelength  $\lambda_B = 2n_{\text{eff}}\Lambda$ , as seen in Fig. 1(a). However, if a longitudinal acoustic wave is excited along the fiber axis  $z$ , it produces a periodic strain, which compresses and stretches the grating. Therefore, the strain modulates the mode effective index  $n_{\text{eff}}(z)$  and the grating period  $\Lambda(z)$ , causing lobes to appear on both sides of the Bragg wavelength [see Fig. 1(b)]. The normalized side lobe reflectivity  $\eta$  is given as [9], [10]

$$\eta = \tanh^2 \left[ \frac{\pi \Delta n_{ac} \Gamma}{\lambda_B} L J_m \left( \frac{\lambda_a}{\Lambda} S \right) \right] \quad (1)$$

where  $S$  is the peak strain,  $J_m$  is the Bessel function of the first kind of order  $m$ ,  $\Delta n_{ac}$  is the grating index modulation amplitude,  $L$  is the grating length,  $\lambda_a$  is the acoustic period, and  $\Gamma$  is

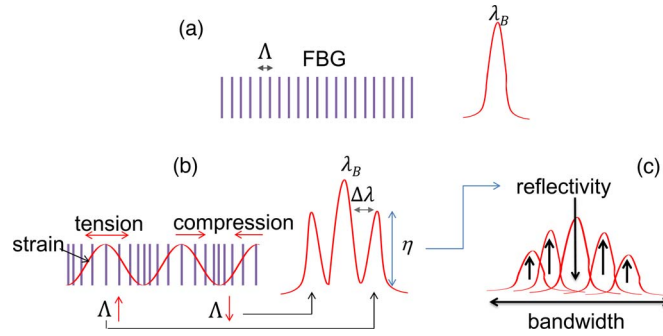


Fig. 1. Behavior of the fiber Bragg grating (a) without and (b) with longitudinal acousto-optic modulation. (c) Reflectivity and bandwidth modulation caused by the acoustic wave.

the fraction of the optical power in the propagating mode that overlaps with the grating. For the step index single mode optical fiber (SMF) the peak strain  $S$  can be approximated as

$$S = \sqrt{\frac{2P_{ac}}{EA_s v}} \quad (2)$$

in which  $P_{ac}$  is the acoustic power,  $E$  is the Young's modulus,  $A_s$  is the silica fiber cross section, and  $v$  is the acoustic velocity. For a specific value of  $P_{ac}$ , it should be noted that in equations (1) and (2) the reflectivity  $\eta$  can be increased by increasing the index modulation  $\Delta n_{ac}$  or the grating length  $L$ , as well, by reducing the fiber diameter. The side lobe separation  $\Delta\lambda$  can be described as [9]

$$\Delta\lambda = \frac{f\lambda_B^2}{2n_{eff}v} \quad (3)$$

which is related with the acoustic frequency  $f$ , the Bragg wavelength  $\lambda_B$ , the acoustic velocity  $v$ , and the effective index  $n_{eff}$ . For weak gratings, the  $m$  order side lobe  $\lambda_m$  has an effective full width at half maximum (FWHM) bandwidth written as

$$\lambda_{mFWHM} = \frac{1.39\lambda^2}{\pi L n_{eff}} \quad (4)$$

Note in (3) that the decrease of frequency  $f$  reduces the distance between the side lobes, while the reduction of the grating length  $L$  in (4) increases the side lobe bandwidth. For frequencies in the order of kHz and short gratings, this combined effect makes the side lobes to overlap each other, which results in a broader grating spectrum.

Previous works have demonstrated that the Bragg resonance reflectivity can be reduced by increasing the acoustic power or, in other words, the reflected light in the resonance can be coupled to higher order side lobes [9]–[11]. As a result, the total grating reflectivity is reduced and the spectrum bandwidth is broader, as illustrated in Fig. 1(c). Current works have revealed that the grating bandwidth can also be increased by a complex superposition of flexural and longitudinal acoustic waves [15]. However, the resultant effect is similar to that caused by a longitudinal acoustic wave.

### 3. Experimental Setup

Fig. 2 shows a cross section of the SCF model IPHT-256b3 fabricated at the Institute of Photonic Technology used in the experiment. The fiber is composed of four air holes of  $D \sim 24 \mu\text{m}$  in diameter separated by silica bridges of  $t \sim 700 \text{ nm}$  thickness, which form a solid core of  $d = 5 \mu\text{m}$  incircle diameter. The fiber cross section diameter is  $\varphi = 100 \mu\text{m}$ .

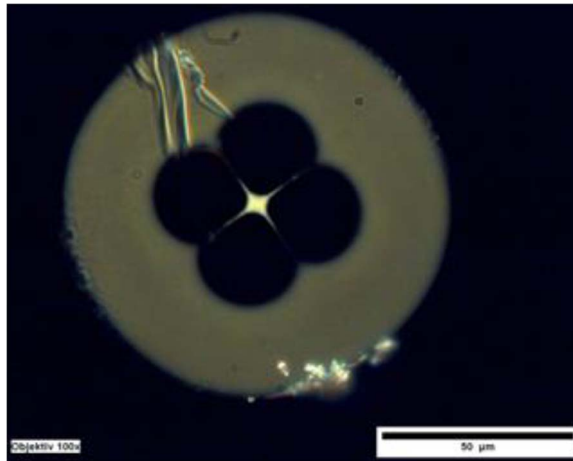


Fig. 2. Cross section of the four air holes suspended core fiber IPHT-256b3 used in the experiment.

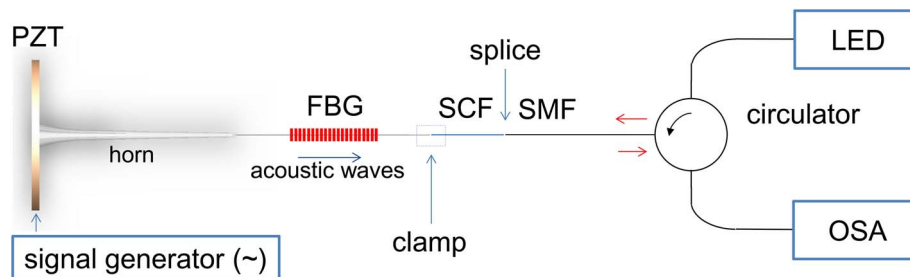


Fig. 3. Experimental setup with the acousto-optic modulator and devices used to characterize the FBG modulated spectrum.

Fig. 3 illustrates the experimental setup used for the characterization of the modulated FBG spectrum. The acoustic waves are excited by an acousto-optic modulator, which is composed of a piezoelectric transducer (PZT disc of 2 mm thick with diameter of 25 mm), a 5 cm long acoustic silica horn and the SCF with the inscribed FBG. The grating is illuminated by a LED and the reflection spectrum is obtained through a circulator and an optical spectrum analyzer (OSA) with a 50 pm wavelength resolution. The light coupling between the SCF and SMF at the circulator is done by splicing the fibers using an arc-discharge fusion splicer (Sumitomo F36) and a modified method to prevent the collapse of the core and the bridges [22]. The fiber is aligned using micrometer XYZ positioning tables to avoid the presence of stress and the Bragg wavelength shift is also monitored during the alignment. The experimental setup is built on a table with a vibration absorption system based on compressed air to reduce mechanical noises from the environment. By fixing the PZT base and the fiber tip, the modulator works as a resonant acoustic cavity that allows exciting standing acoustic waves at certain resonant frequencies.

We inscribed a narrow and a broad bandwidth FBG of 1 cm length by means of a femtosecond laser and two-beam interference using the Talbot interferometer arrangement according to the methodology described in [17] and [23]. For each grating, different fiber lengths and frequencies are used in the setup of Fig. 3.

For the narrow bandwidth grating, the 3-dB bandwidth is 0.26 nm and the maximum reflectivity is  $\sim 99\%$  with a SCF length of 5 cm. The PZT is excited by 1–9 V sinusoidal signal from an arbitrary signal generator at  $f = 216$  kHz, 343 kHz, 360 kHz and 497 kHz, respectively. The changes in the grating reflectivity are observed to be stronger for these frequencies, due mainly to the PZT resonances and the matching between the acoustic wavelengths and the horn-fiber length.

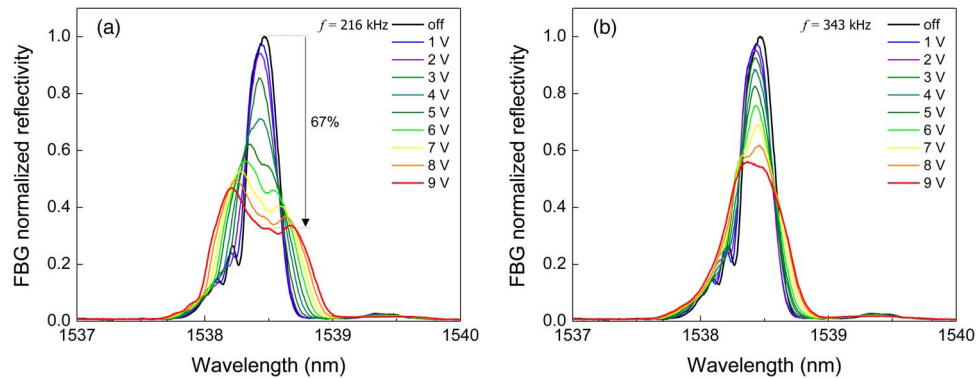


Fig. 4. Modulated FBG spectra at (a)  $f = 216$  kHz and (b) 343 kHz.

The broad bandwidth grating has  $\sim 1$  nm 3-dB bandwidth and the maximum reflectivity is 99.9% with a SCF length of 4.5 cm. The PZT is excited by 1–10 V maximum voltage at  $f = 282$  kHz. For other frequencies, no relevant effect is observed.

#### 4. FBG Reflectivity Modulation

Fig. 4(a) and (b) shows the modulated FBG spectra for the acoustic resonances at  $f = 216$  kHz and 343 kHz, for which the reflectivity variations are strong. The changes in the reflectivity amplitude for all resonances are monitored when 1 to 9 V are applied to the PZT. The bandwidth modulation is not evaluated for this grating since the spectrum changes asymmetrically from the Gaussian shape at  $f = 216$  kHz. The spectra are normalized in relation to the maximum reflectivity at  $\lambda_B = 1538.46$  nm for the case where no acoustic wave is present. The reflectivity variations for all the modulated spectra are evaluated only at this wavelength. Fig. 4(a) shows the reflectivity changes for the resonance at  $f = 216$  kHz. The reflectivity at the Bragg resonance is reduced almost uniformly in the 1 to 4 V voltage range without considerable changes in the spectrum shape. This behavior is also observed for the resonance at  $f = 343$  kHz in Fig. 4(b). However, the reflectivity amplitude at  $f = 216$  kHz is reduced considerably in the 5–9 V voltage range and the spectrum bandwidth becomes wider. The reflectivity is reduced from 100 to 33% (67% reduction), and the 3-dB bandwidth increases from 0.26 to 0.74 nm when 9 V voltages are applied to the PZT. However, the side lobes that compose the wider bandwidth are not resolved in the FBG spectrum. According to (3) the side lobe separation,  $\Delta\lambda$ , is small ( $\Delta\lambda = 31 - 71$  pm) for the frequency range evaluated ( $f = 216-497$  kHz). Therefore, the side lobes overlap each other and compose the wider spectrum. Note in the spectrum that the side lobe reflectivity is higher for the shorter wavelength range. This is because the grating without modulation already has intrinsic lobes on the left side. The FBG fabricated using the femtosecond laser is not apodized. The side lobes on the short wavelength of the Bragg resonance are caused mainly by the non-uniform average refractive index along the grating resultant from the inscription process and influence of overlapped higher order modes [23]. As a result, the overlap between these grating lobes and the acoustic induced lobes cause higher reflectivity on the left side of the Bragg resonance, which makes the modulated FBG to have an asymmetric spectrum. If a grating with relatively symmetrical spectrum is used, the modulated spectrum is also expected to have a more symmetrical shape [15].

Fig. 5(a) shows the FBG reflectivity behavior of resonances for a set of voltages applied to the PZT. Note that the reflectivity decrease is the largest for the resonance at  $f = 216$  kHz. The 5 cm fiber length is also resonant with two longitudinal acoustic wavelengths of  $\lambda_a = 2.6$  cm, which contributes to reinforce the interaction. This effect is also seen in Fig. 5(b) for the frequency response. The effect is reduced for higher frequencies mainly because the PZT deformations are also reduced with the increase of frequency [12]. The higher frequency also reduces the acoustic wavelength, which naturally decreases the side lobe reflectivity according to (1).

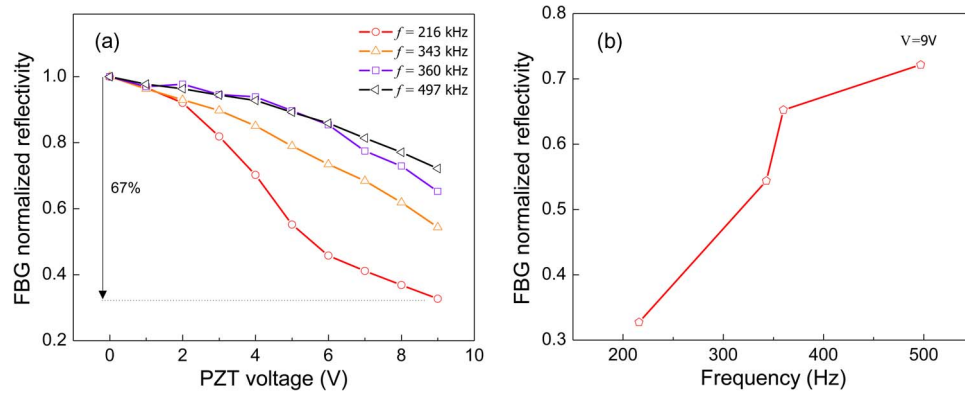


Fig. 5. Modulated FBG reflectivity for (a) the PZT voltage and (b) frequency responses.

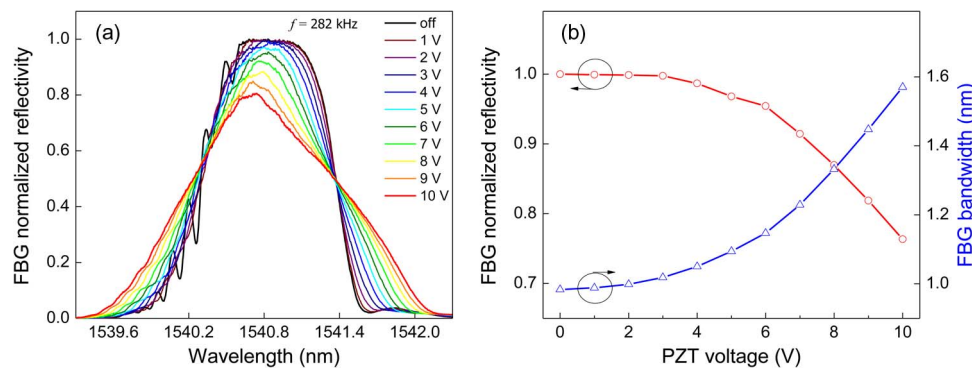


Fig. 6. (a) Modulated FBG spectra at  $f = 282$  kHz and (b) FBG reflectivity amplitude (red) and 3-dB bandwidth (blue) for 1–10 V voltage range applied to PZT.

The modulated reflectivity achieves saturation at about  $f = 500$  kHz and no relevant effect is observed after this frequency.

We verified from previous works that similar results have been obtained by using a SMF and a similar setup [24]. The grating inscribed in the SMF is 2 cm long, and the PZT is excited at 230 kHz. A RF signal amplifier is used to increase the voltage range applied to the PZT from 0 to 150 V. The maximum side lobe reflectivity decrease obtained is 68% at 150 V. In comparison, we obtained a similar maximum modulation of 67% as seen in Fig. 5(a) at 216 kHz. However, the grating inscribed in the SCF is 1 cm long (half the grating than SMF), and the voltage used is 9 V ( $16\times$  lower than the voltage applied in the SMF modulator). In summary, these previous results points out possibilities to reduce the size and the power consumed by acousto-optic devices compared to standard fibers.

## 5. FBG Bandwidth Modulation

Fig. 6(a) shows the modulated spectrum for the broad bandwidth grating for the acoustic resonance at  $f = 282$  kHz, where stronger reflectivity variations are observed. The spectra are normalized in relation to the maximum reflectivity at  $\lambda_B = 1540.83$  nm for the case without acoustic wave. The reflectivity amplitude and bandwidth variations for all the modulated spectra are evaluated only at this wavelength. The grating without modulation already has also intrinsic lobes on the left side, which are probably due to the high reflectivity of the grating and influence of higher modes. However, with application of the acoustic wave, the spectrum shape is changed to an almost Gaussian shape. Fig. 6(b) shows that the reflectivity amplitude is reduced from 100% to 76% (24% decrease) and the 3-dB bandwidth is increased from 1 to 1.57 nm (57% increase),

for the 1–10 V voltage range applied to the PZT. The side lobes that compose the wider bandwidth are also not resolved in the FBG spectrum as predicted.

## 6. Conclusion

In conclusion, the acousto-optic modulation of fiber Bragg gratings in a four holes suspended core fiber is demonstrated. The reflectivity amplitude and the bandwidth of different gratings are investigated under acoustic excitation.

For the narrow bandwidth grating, the Bragg resonance reflectivity amplitude is adjustable by the amplitude voltage of an electrical signal. The reflectivity can be decreased by up to 67% at  $f = 216$  kHz. The response efficiency (reflectivity/voltage) can be improved by optimizing the modulator design, optical fiber and inscribed Bragg grating, and adjusting the frequency and amplitude of the resultant acoustic wave.

For the broad bandwidth grating, the bandwidth can be increased by up to 57% while keeping considerable reflectivity amplitude (76%). In addition, the spectrum envelope can be corrected to an almost Gaussian shape, which is useful for applications such as tunable filters and dispersion compensators.

In general, the SCF allows higher modulation efficiency compared to a solid SMF, which can be useful to reduce the modulator size and the energy required to excite the acoustic waves. Moreover, the SCF provides better mechanical stability compared to fiber taper techniques and protects the acoustic wave in the core, due to acoustical shielding by the cladding against external acoustic noise. Thus, the acousto-optic effect in suspended-core fibers indicates possibilities of more efficient fiber-based acousto-optic modulators.

---

## References

- [1] A. A. P. Pohl, K. Cook, and J. Canning, "Acoustic-induced modulation of photonic crystal fiber Bragg gratings," in *Proc. Conf. Transp. Opt. Netw.*, 2008, pp. 51–54.
- [2] J. H. Lee *et al.*, "Wavelength and repetition rate tunable optical pulse source using a chirped fiber Bragg grating and a nonlinear optical loop mirror," *IEEE Photon. Technol. Lett.*, vol. 17, no. 1, pp. 34–36, Jan. 2005.
- [3] I. C. M. Littler, M. Rochette, and B. J. Eggleton, "Adjustable bandwidth dispersionless bandpass FBG optical filter," *Opt. Exp.*, vol. 13, no. 3, pp. 3397–3407, May 2005.
- [4] B. Dabarsyah *et al.*, "Adjustable group velocity dispersion and dispersion slope compensation devices with wavelength tunability based on enhanced thermal chirping of fiber Bragg gratings," *J. Lightw. Technol.*, vol. 25, no. 9, pp. 2711–2718, Sep. 2007.
- [5] J. Kim *et al.*, "Effectively tunable dispersion compensation based on chirped fiber Bragg gratings without central wavelength shift," *IEEE Photon. Technol. Lett.*, vol. 16, no. 3, pp. 849–851, Mar. 2004.
- [6] C. S. Goh, S. Y. Set, and K. Kikuchi, "Design and fabrication of a tunable dispersion-slope compensating module based on strain-chirped fiber Bragg gratings," *IEEE Photon. Technol. Lett.*, vol. 16, no. 2, pp. 524–526, Feb. 2004.
- [7] Y. Y. J. Lee, J. Bae, K. Lee, J.-M. Jeong, and S. B. Lee, "Tunable dispersion and dispersion slope compensator using strain-chirped fiber Bragg grating," *IEEE Photon. Technol. Lett.*, vol. 19, no. 10, pp. 762–764, May 2007.
- [8] P. T. Neves and A. A. P. Pohl, "Time analysis of the wavelength shift in fiber Bragg gratings," *J. Lightw. Technol.*, vol. 25, no. 11, pp. 3580–3588, Nov. 2007.
- [9] W. F. Liu, P. S. J. Russell, and L. Dong, "100% efficient narrow-band acoustooptic tunable reflector using fiber Bragg grating," *J. Lightw. Technol.*, vol. 16, no. 11, pp. 2006–2009, Nov. 1998.
- [10] S. J. Russell and W. F. Liu, "Acousto-optic superlattice modulation in fiber Bragg gratings," *Opt. Soc. Amer. A.*, vol. 22, no. 19, pp. 1515–1517, Oct. 2000.
- [11] M. Delgado-Pinar, D. Zalvidea, A. Diez, P. Perez-Millan, and M. Andres, "Q-switching of an all-fiber laser by acousto-optic modulation of a fiber Bragg grating," *Opt. Exp.*, vol. 14, no. 3, pp. 1106–1112, Feb. 2006.
- [12] R. E. Silva, M. A. R. Franco, H. Bartelt, and A. A. P. Pohl, "Numerical characterization of piezoelectric resonant transducer modes for acoustic wave excitation in optical fibers," *Meas. Sci. Technol.*, vol. 24, no. 9, Sep. 2013, Art. ID. 094020.
- [13] R. E. Silva, M. A. R. Franco, P. T. Neves, H. Bartelt, and A. A. P. Pohl, "Detailed analysis of the longitudinal acousto-optical resonances in a fiber Bragg modulator," *Opt. Exp.*, vol. 21, no. 6, pp. 6997–7007, Mar. 2013.
- [14] R. A. Oliveira, P. T. Neves, J. T. Pereira, and A. A. P. Pohl, "Numerical approach for designing a Bragg grating acousto-optic modulator using the finite element and the transfer matrix methods," *Opt. Comm.*, vol. 281, no. 19, pp. 4899–4905, Oct. 2008.
- [15] A. A. P. Pohl, R. E. Silva, M. A. R. Franco, P. T. Neves, and H. Bartelt, "Modelling the bandwidth behaviour of fibre Bragg gratings excited by low-frequency acoustic waves," in *Proc 15th ICTON*, 2013, pp. 1–4.
- [16] K. Hill and G. Meltz, "Fiber Bragg grating technology fundamentals and overview," *J. Lightw. Technol.*, vol. 15, no. 8, pp. 1263–1276, Aug. 1997.
- [17] M. Becker *et al.*, "Fiber Bragg grating inscription combining DUV sub-picosecond laser pulses and two-beam interferometry," *Opt. Exp.*, vol. 16, no. 23, pp. 19169–19178, Nov. 2008.

- [18] M. Phan Huy *et al.*, "Three-hole microstructured optical fiber for efficient fiber Bragg grating refractometer," *Opt. Lett.*, vol. 32, no. 16, pp. 2390–2392, Aug. 2007.
- [19] S. V. Afshar, S. Warren-Smith, and T. Monro, "Enhancement of fluorescence-based sensing using microstructured optical fibres," *Opt. Exp.*, vol. 15, no. 26, pp. 17 891–17 901, Dec. 2007.
- [20] L. Fu, B. Thomas, and L. Dong, "Efficient supercontinuum generations in silica suspended core fibers," *Opt. Exp.*, vol. 16, no. 24, pp. 19 629–19 642, Nov. 2008.
- [21] A. Hartung, A. Heidt, and H. Bartelt, "Pulse-preserving broadband visible supercontinuum generation in all-normal dispersion tapered suspended-core optical fibers," *Opt. Exp.*, vol. 19, no. 13, pp. 12 275–12 283, Jul. 2011.
- [22] Y. Wang *et al.*, "Splicing Ge-doped photonic crystal fibers using commercial fusion splicer with default discharge parameters," *Opt. Exp.*, vol. 16, no. 10, pp. 7258–7263, May 2008.
- [23] M. Becker *et al.*, "Inscription of fiber Bragg grating arrays in pure silica suspended core fibers," *IEEE Photon. Technol. Lett.*, vol. 21, no. 19, pp.1453–1455, Oct. 2009.
- [24] R. A. Oliveira, P. T. Neves Jr., J. T. Pereira, J. Canning, and A. A. P. Pohl, "Vibration mode analysis of a silica horn fiber Bragg grating device." *Opt. Commun.*, vol. 283, no. 7, pp. 1296–1302, Apr. 2009.